

## FEA comparison of high and low pressure tube hydroforming of TRIP steel

C. Nikhare\*, M. Weiss, P.D. Hodgson

*Institute for Technology Research and Innovation, Deakin University, Waurn Ponds 3217, Australia*

### ARTICLE INFO

#### Article history:

Received 4 April 2009

Received in revised form 29 May 2009

Accepted 30 June 2009

Available online 26 July 2009

#### Keywords:

Hydroforming

Low pressure

High pressure

AHSS

Friction

### ABSTRACT

The increasing application of hydroforming for the production of automotive lightweight components is mainly due to the attainable advantages regarding part properties and improving technology of the forming equipment. However, the high pressure requirements during hydroforming decreases the costs benefit and make the part expensive. Another requirement of automotive industries is weight reduction and better crash performance. Thereby steel industries developed advanced high strength steels which have high strength, good formability and better crash performance. Even though the thickness of the sheet to form the component is reduced, the pressure requirement to form the part during expansion is still high during high pressure hydroforming. This paper details the comparison between high and low pressure tube hydroforming for the square cross-section geometry. It is determined that the internal pressure and die closing force required for low pressure tube hydroforming process is much less than that of high pressure tube hydroforming process. The stress and thickness distribution of the part during tube crushing were critically analysed. Further, the stress distribution and forming mode were studied in this paper. Also friction effect on both processes was discussed.

Crown Copyright © 2009 Published by Elsevier B.V. All rights reserved.

### 1. Introduction

The automotive industry is increasingly interested in mass reduction of vehicles for improved fuel consumption. Hydroforming is a metal forming process that is now widely used as it can achieve weight reduction of about 30% compared to conventionally manufactured components [1]. At the same time automakers are increasingly exploring the potential to use advanced high strength steels, as they can also provide weight reduction without any reduction in other performance characteristics such as crash and durability.

The tube hydroforming process can be categorised into three pressurization systems: (1) low pressure hydroforming ( $P < 83$  MPa) (2) multipressure hydroforming ( $P = 69$ – $173$  MPa) and (3) high pressure hydroforming ( $P = 83$ – $414$  MPa) [2]. Most research to date has focussed on high pressure hydroforming, particularly to improve the quality of the product and formability. For example local thinning and wrinkling can be prevented by oscillating the internal pressure in pulsating hydroforming. Through oscillations of the internal pressure, a uniform expansion in the bulging region was obtained, and thus the formability was improved by preventing the local thinning [3]. Accumulation of material in the expanding area by formation of useful wrinkles instead of dead wrinkles is an effective method to achieve good formability. This gives the modified process window for without wrinkles and

useful wrinkles for hydroforming [4]. Yuan et al. [5] studied the influence of wrinkling behaviour on formability and thickness distribution in THF. Jain and Wang [6] developed a dual-pressure tube hydroforming process in which the plastic instability is delayed and the ductility of the metal is increased. Smith et al. [7] investigated tube hydroforming with a double-sided high pressure (DSHP) boundary condition which increased formability relative to that observed for the traditional single-sided high pressure (SSHP). To enhance the formability in whole tube hydroforming process, the feasible preform design method based on deformation history during forward loading was introduced [8]. Thinning values were compared to the simulation in order to validate the finite element model for the process. The FE model correctly predicts the THF process in terms of part shape and thinning distribution and hence simulation is a valid tool for such feasibility studies [9]. Different loading paths were studied to improve the formability of the tube [10]. Some of the literature has studied the effect of friction [11] on formability and an analytical model [12] to determine the friction coefficient was developed. According to the model, the friction coefficient can be calculated using the geometrical data from the deformed tube and materials properties without a force measurement.

There have been a number of studies by FEA to predict wrinkling, necking and bursting and compare with the experimental results [4,5,13–20]. Asnafi and Skogsgardh [21] proposed stroke controlled hydroforming to avoid the risk of buckling and fracture. Forming limit strains for loading with specifies fluid volumes are higher when compared to those with prescribed fluid pressure.

\* Corresponding author. Tel.: +61 352272235; fax: +61 352271103.

E-mail addresses: [cpni@deakin.edu.au](mailto:cpni@deakin.edu.au), [chetan.nikhare@gmail.com](mailto:chetan.nikhare@gmail.com) (C. Nikhare).

Thus better formability may be attained in tube hydroforming by prescribing the fluid volume instead of pressure, in conjunction with axial feed [13]. Controlled forming pressure and end feed were applied to accurately form the tube. Faster pressure application compared to axial feed leads to excessive thinning and bursting, or fracture due to crack growth [14,16–20]. Combined internal pressure and axial feeding applied on X and T branch components [15,22] for anisotropic materials showed that the bursting pressure is increased with respect to an increase in anisotropic parameter *R*-value.

In comparison the research performed on low pressure hydroforming is limited and there is still insufficient knowledge to how effective design with the process. However, one of the attractions of this process is that it requires much lower pressures and it is of note that the high pressures above were for simple low carbon structural steels. For the advanced high strength steels the stresses required to deform the metal are much higher and hence the pressure requirements are further increased.

In this paper, a numerical comparison between low and high pressure tube hydroforming was carried out for the same final component. A ramp pressure curve was applied during the high pressure process, which allows a linear variation to the desired pressure with respect to time until the tube was completely formed. A constant pressure was applied for low pressure hydroforming. The die closing forces to form the tube were predicted along with the stress and thickness distribution. Further effect of friction for both processes was studied.

**2. Material and methodology**

**2.1. Material**

The steel used for the numerical investigation of the high and low pressure tube hydroforming processes was a commercial TRIP 780 grade. The true stress–strain curve determined in a conventional tensile test and used for simulation is shown in Fig. 1, while the mechanical properties are given in Table 1.

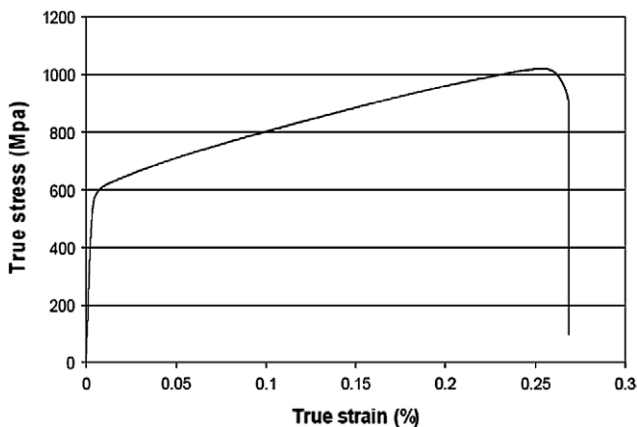


Fig. 1. True stress–strain curve determined in tensile tests for TRIP steel.

**2.2. Methodology**

In this study the high pressure tube hydroforming (HPTH) and low pressure tube hydroforming (LPTH), shown in Figs. 2 and 3,

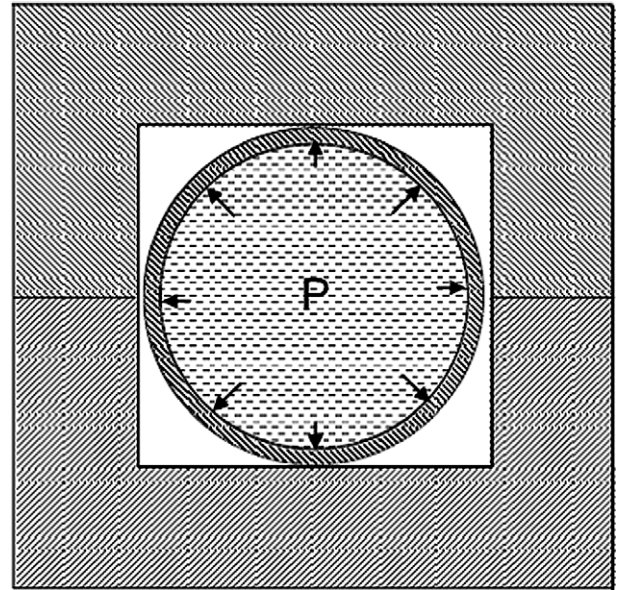


Fig. 2. Start of high pressure tube hydroforming (HPTH).

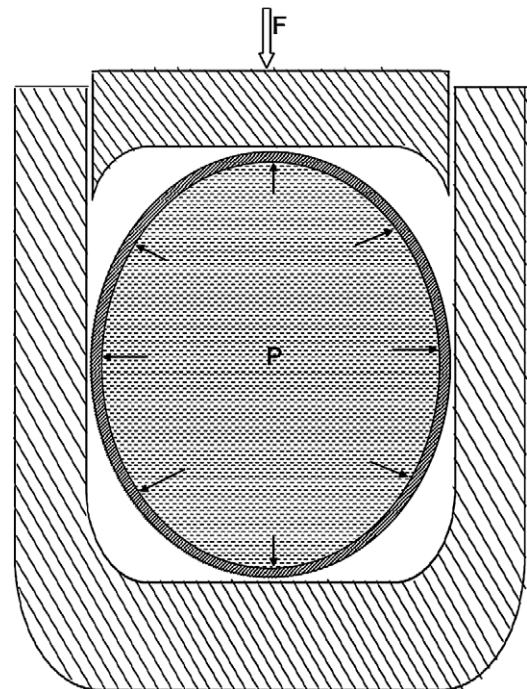


Fig. 3. Preform tube and start of low pressure tube hydroforming (LPTH).

**Table 1**  
Mechanical properties of TRIP steel.

Designation	Mechanical properties				
	Yield strength (MPa)	Tensile strength (MPa)	Elongation (%)	<i>K</i> (MPa)	<i>n</i>
TRIP (780 grade)	550	1020	26	1365	0.2263

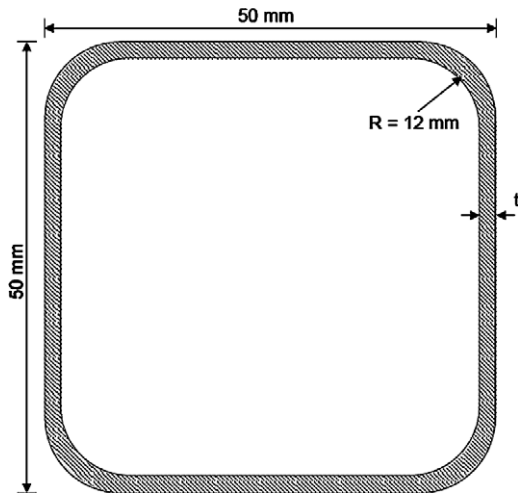


Fig. 4. Final part with dimensions.

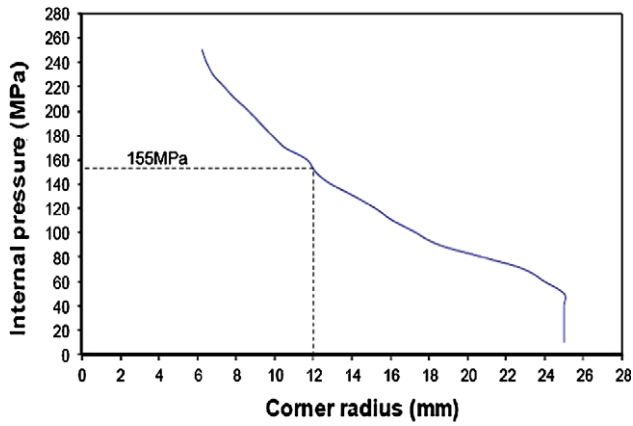


Fig. 5. Internal pressure versus tube corner radius during high pressure tube hydroforming.

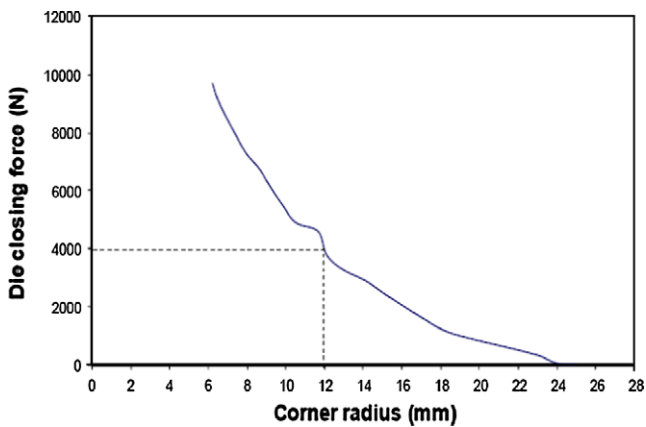


Fig. 6. Force curve for different formed tube corner radius.

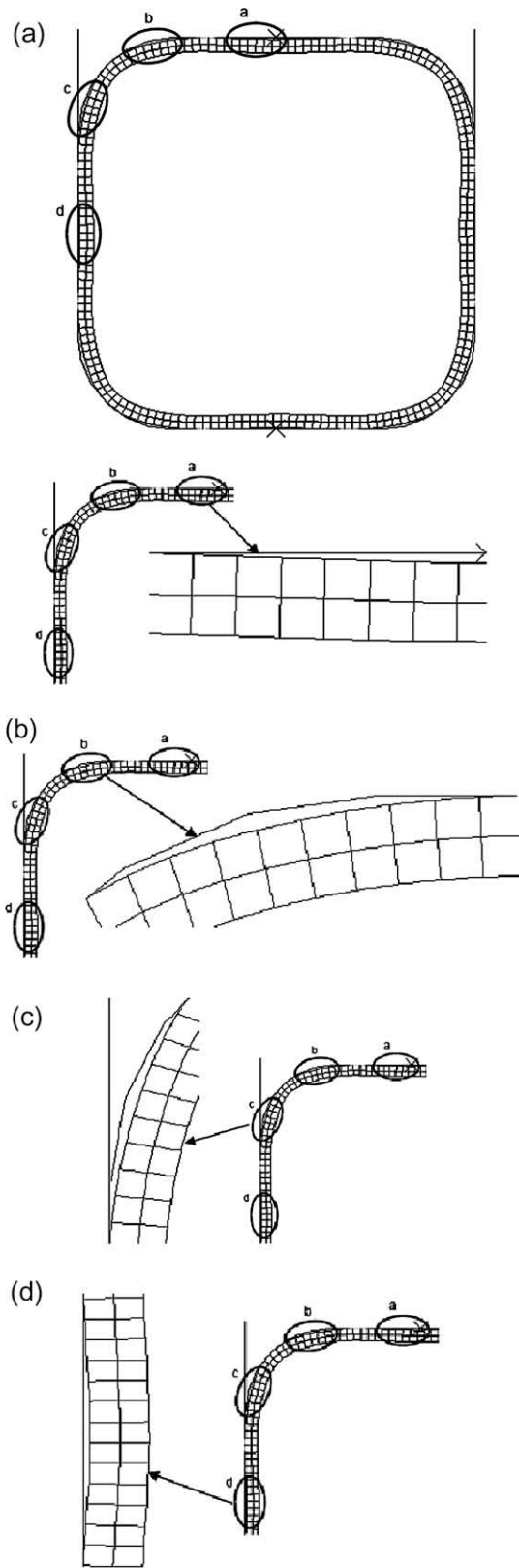


Fig. 7. Tube formed using LPTH with a fluid pressure of  $P = 0$  MPa and showing major shape imperfections.

were investigated and compared using a numerical model. Thereby the die filling conditions as well as the forming pressures and the die closing forces of both processes was analysed and compared

for the forming of the same tube shape. Additionally the stress and thickness distributions over the tube wall were analysed and the effect of friction in both processes was compared.

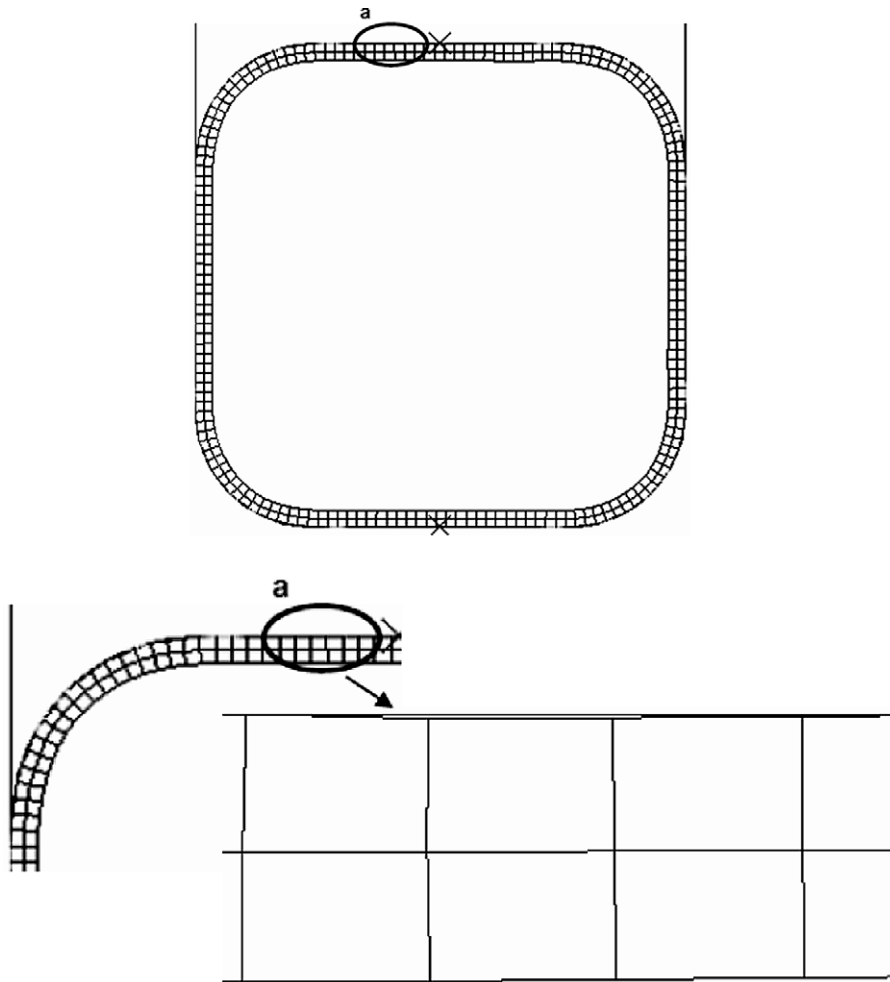


Fig. 8. Tube formed using LPTH with a fluid pressure of  $P = 10$  MPa and showing only small shape imperfections.

### 2.2.1. High pressure tube hydroforming (HPTH)

The tubular part deformed in the stretch mode by applying the high pressure is designated as HPTH. The most common tube hydroforming set up is shown in Fig. 2. The tube is placed in the fixed lower die and the upper die moves down to close the gap. After closing the dies, the tube is filled with incompressible fluid and pressurised to form the desired shape. Thereby the tube material is stretched and fills the die corners.

### 2.2.2. Low pressure tube hydroforming (LPTH)

In LPTH, the tube is formed to the desired shape using relatively low fluid pressures. For this the tube is placed between the upper and lower die. The lower die is fixed while the upper die moves down and forms the tube which is filled and pressurised incompressible fluid.

In LPTH, the circular perimeter of the undeformed tube must be equal to the perimeter of the final part. Thus, the perimeter of the outer undeformed tube must be the same as that of the inner perimeter of the die. The process is shown in Fig. 3.

### 2.2.3. Numerical modelling

The forming of the square geometry shown in Fig. 4 was simulated for both the HPTH and the LPTH processes using the commercial software package ABAQUS/Explicit 6.5-1. The tube was assumed to be a perfectly circular cylinder and variations in wall thickness or material properties around the circumference of the tube were neglected. Two tube thicknesses were investigated in

this work. The wall thickness of the initial, round tube was taken to be 2 mm in the HPTH process and 1.75 mm (i.e. minimum thickness of the final product during high pressure) in the LPTH process. In this way the overall material requirement was the same for both forming processes. In the numerical model, the cylindrical length was considered to be 1 mm while the outside diameter of the undeformed tube was 50 mm in the HPTH process and 57.12 mm in LPTH. Tensile true stress–strain data (Fig. 1) was used to define the material properties. The die was considered to be rigid while the tube was defined to be deformable. Two layers of CPE4R 4-node bilinear plane strain elements were used through the material thickness. The tube was allowed to radially expand and compress and the interaction between die and the tube was assumed to be frictionless. For comparison a model using friction (coefficient of friction = 0.1) was also performed. Internal pressure and the movement of upper die were applied simultaneously.

## 3. Results and discussion

### 3.1. High pressure tube hydroforming

The filling of the corner radii with respect to the internal pressure is shown for HPTH in Fig. 5. Up to 50 MPa internal fluid pressure, the tube material does not deform plastically. With higher pressure, the tube starts deforming and continuously fills the die corner radius, i.e. with an increase in pressure, the corner radius of the tube decreases. The plot of internal pressure versus corner

radii appear to be hyperbolic, i.e. the internal pressure is inversely proportional to the corner radius, but it involves the thickness effect. The idea to plot the curve determines the pressure during HPTH where a 12 mm corner radius is obtained. The die closing force requirement for the particular corner radius is shown in Fig. 6 which shaped as hyperbola instead of linear, as the projected area was continuously increased during the process.

The internal tube pressure required to form the final shape is 155 MPa which is comparable through calculation from analytical equation [2].

### 3.2. Low pressure tube hydroforming

The LPTH was analysed for internal tube pressures of 0 and 10 MPa. Fig. 7 shows the final shape of the tube after forming with an internal tube pressure of 0 MPa. The formed product has non-contact regions with the die. The circles in the figure highlight the non-contact regions, which are exaggerated in Fig. 7a–d.

When formed with an internal tube pressure of 10 MPa the material obtain the desired shape with only slight imperfections visible in the top and bottom walls (Fig. 8). Hence in LPTH, an internal pressure of 10 MPa is sufficient to obtain the final part while to form the same part shape in HPTH a fluid pressure of 155 MPa would be required. Table 2 compares the fluid pressures and the die closing force required in both tube forming processes and the percentage reduction of magnitude in low pressure compared to high pressure for the geometry.

The prediction of stress and thickness distribution over the tube was obtained for a vertical half symmetry. The direction for prediction of results is given in Fig. 9.

**Table 2**  
Fluid pressures and holding forces determined for the HPTH and the LPTH process.

Parameter	Process		% Reduction
	High pressure	Low pressure	
Pressure (MPa)	155	10	93.5
Holding force (N)	4000	2300	42.5

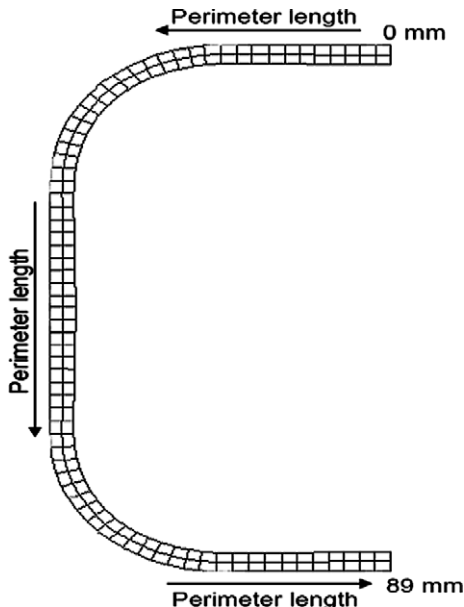


**Fig. 9.** Half formed tube indicating the direction for prediction of stress and thickness.

The average von-Mises stresses in the tube wall during high and low pressure hydroforming are shown in Fig. 10. Positive wall stresses are generated during high pressure tube hydroforming while negative stresses are observed for the case of LPTH. This indicates that in HPTH the tube elements are stretched during forming while in LPTH the material is compressed. The stresses in the corners are less than elsewhere in the part during HPTH, while this is the opposite case for low pressure and the number of elements involved (i.e. length of tube) is much lower.

In Fig. 11 the thickness distributions along the tube perimeter are shown for both tubes. Due to the differences in initial wall thickness, in Fig. 11 the wall thickness distributions are given in the form of the relative thickness; this is the ratio of the wall thickness of the formed part to the wall thickness of the initial undeformed tube. In Fig. 11 it is clear that the tube is thinning in HPTH while in low pressure the variation is negligible. The figure indicates that, if the initial tube thickness is 1 mm, the tube is thinning in HPTH while it remains constant in LPTH with a slight variation.

The tube is thinning non-uniformly along the circumference in the case of HPTH, with the corners thinning less than the other part of the tube. As soon as the tube element comes in contact with die,

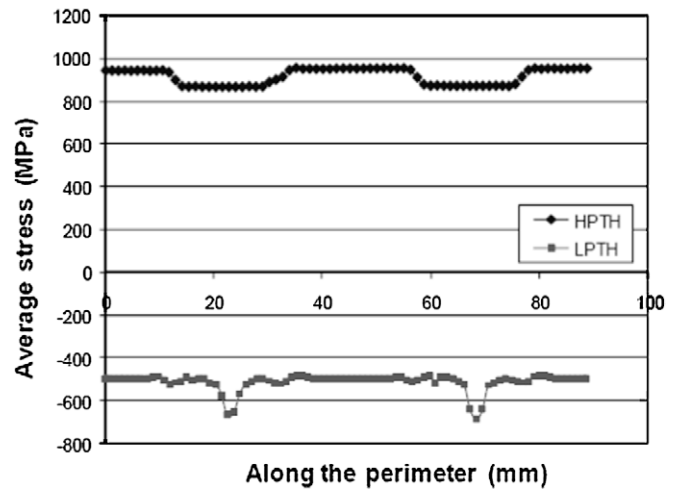


**Fig. 10.** Stress distributions in deformed half tube during HPTH and LPTH.

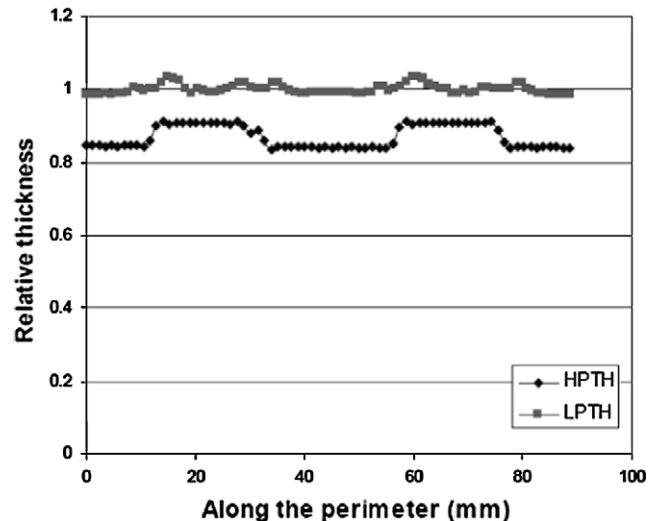


**Fig. 11.** Relative thickness distribution of deformed half tube during HPTH and LPTH.

two forces are acting on the element. One force acting on outer surface is the normal die reaction while the fluid pressure is on the inner surface. The fluid force pushes the material towards the corners. Due to the assumption of frictionless dies, the tube is not sticking to the wall but moves towards the corner and, thereby, the corners are thinning less than the other region.

3.3. Stress distribution and forming mode

In Fig. 12 the tube corner with two sections cuts are shown. In section I, the tube is straightening while in section II, the tube is

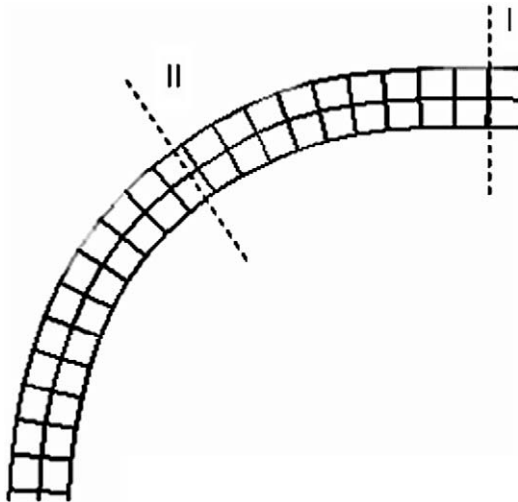


Fig. 12. Quarter formed tube with two analysis section.

bending as a result of the applied internal fluid pressure. The material was assumed to be linear elastic to analyse the forming mode. The tensile forces are acting on elements in both sections during HPTH (Fig. 13). The elements are stretching and hence are in tension. Due to the tensile force, the material is pulling from both sides. Thus the tube is thinning less in corners than the other parts. In the case of LPTH, compressive forces are acting in both sections (Fig. 14). The elements are mostly being bent and compressed. In both processes the forming mode is the same but the stress are opposite in direction with different magnitudes.

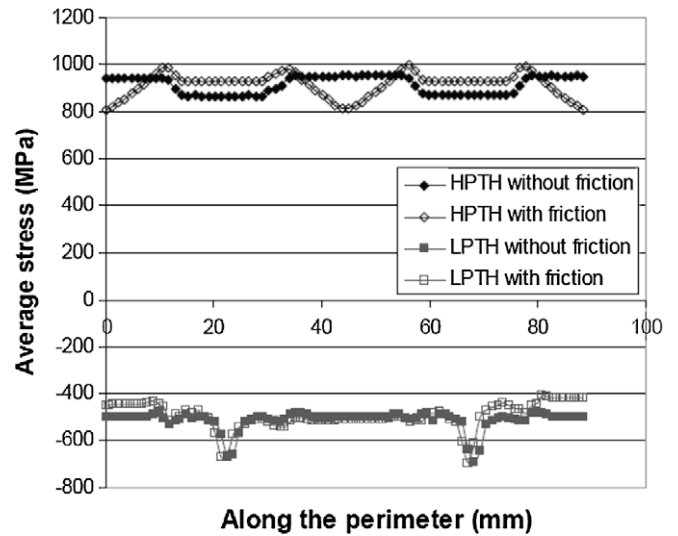


Fig. 15. Stress in deformed half tube during HPTH and LPTH for with and without friction.

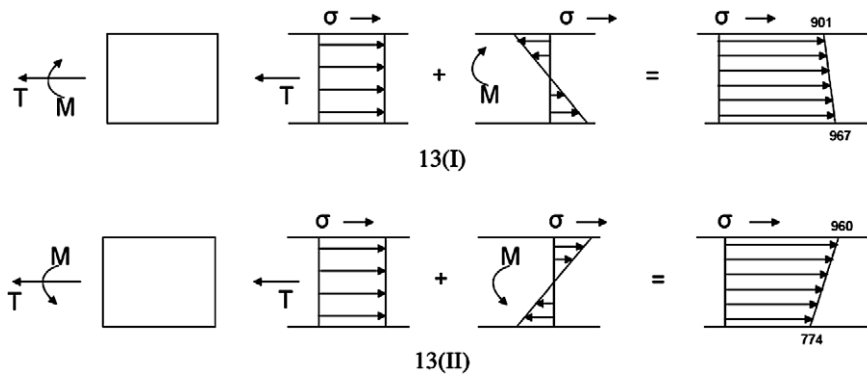


Fig. 13. Stress distributions and forming mode in two sections during tube expansion (HPTH).

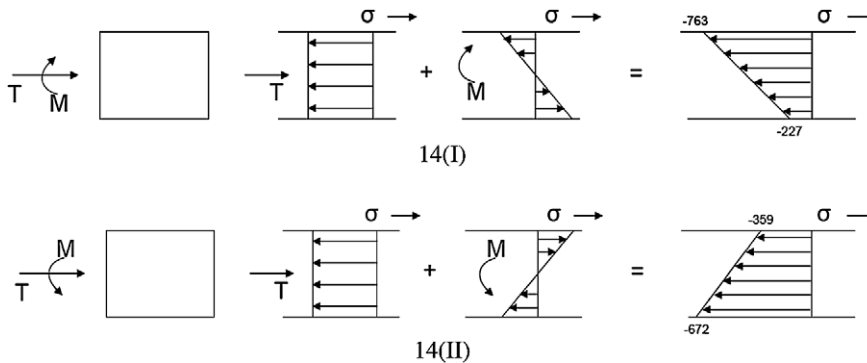


Fig. 14. Stress distributions and forming mode in two sections during tube crushing (LPTH).

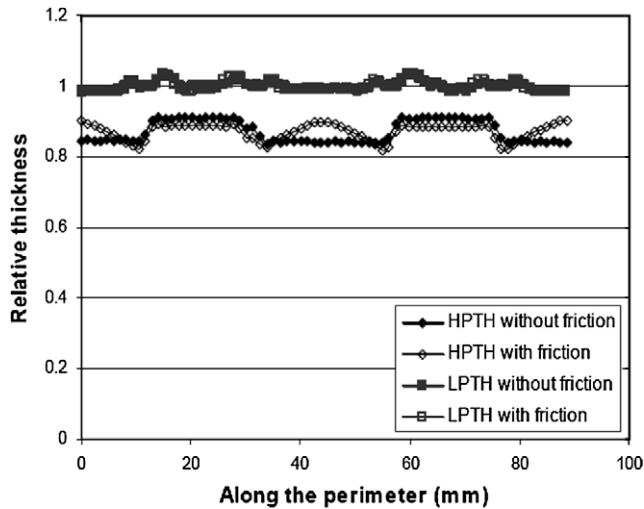


Fig. 16. Relative thicknesses in deformed half tube during HPTH and LPTH with and without friction.

### 3.4. Friction effect

The numerical analysis was repeated for the HPTH and the LPTH (with internal pressure of 10 MPa) processes using a friction coefficient of 0.1. While in HPTH the internal pressure required to form the desired shape increased from 155 to 160 MPa, while in LPTH no effect on the final shape was observed.

The effect of friction on the stress distribution in the tube wall is shown in Fig. 15. It is clear that in HPTH, friction leads to a significant change of the stress profile in the tube wall while only a minor effect of friction can be observed in LPTH. In HPTH without friction, the stress profile takes the path of a trapezoidal waveform with a mean of 900 MPa, but with friction the curve shifts toward higher stress with start of 800 MPa. The stress is increasing from mid of the wall to the start of the corner and then decreases a little and steady for the whole corner radius. This is because the friction restricts the tube material at the middle wall and fluid forces the material to fill the corners, i.e. feeding the material. So the stress is less at the middle and starts increasing towards the corner.

The increased fluctuation of stress with friction observed in HPTH leads to a very inhomogeneous thickness profile (Fig. 16). The HPTH with friction indicates that the material thins more at the start and end of corner radius to fill the die. In contrast to that in LPTH the wall thickness of the formed tube remains constant over the full tube perimeter. The overall trend shows that HPTH is sensitive to friction.

## 4. Conclusion

HPTH and LPTH of TRIP 780 steel for the same final geometry is studied. Using finite element simulation pressure and die closing force are found with respect to corner radius. For the analysed part geometry 155 MPa of internal fluid pressure and 4000 N of die

closing force is required to form the desired shape during HPTH, while only 10 MPa and 2300 N is required in LPTH. The stress variation and thinning is more pronounced in HPTH than in LPTH. LPTH with  $t = 1.75$  mm gives approximate the same thickness distribution that with  $t = 2$  mm in HPTH. Thus weight reduction and uniform thickness distribution are the main advantage during proposed low pressure tube hydroforming. The stress distribution and forming mode are different in both the processes. During high pressure hydroforming the stress and thinning without friction is less than with friction, thus high pressure hydroforming is sensitive to friction while in case of low pressure hydroforming, friction is not an important parameter.

## Acknowledgments

This research was supported by Deakin University. The authors gratefully extend their gratitude to Professor John L. Duncan from Auckland University, New Zealand.

## References

- [1] H.C. Lucke, C. Hartl, T. Abbey, *Journal of Materials Processing Technology* 115 (2001) 87–91.
- [2] H. Singh, *Fundamentals of Hydroforming*, Association for Forming and Fabricating Technologies of the Society of Manufacturing Engineers, Michigan, 2003.
- [3] K. Mori, T. Maeno, S. Maki, *International Journal of Machine Tools and Manufacture* 47 (2007) 978–984.
- [4] S. Yuan, X. Wang, G. Liu, Z.R. Wang, *Journal of Materials Processing Technology* 182 (2007) 6–11.
- [5] S. Yuan, W. Yuan, X. Wang, *Journal of Materials Processing Technology* 177 (2006) 668–671.
- [6] N. Jain, J. Wang, *International Journal of Mechanical Sciences* 47 (2005) 1827–1837.
- [7] L.M. Smith, S. Ganeshmurthy, K. Alladi, *Journal of Materials Processing Technology* 142 (2003) 599–608.
- [8] W.J. Song, S.C. Heo, J. Kim, B.S. Kang, *Journal of Materials Processing Technology* 177 (2006) 658–662.
- [9] E. Ceretti, C. Contri, C. Giardini, *Journal of Materials Processing Technology* 177 (2006) 672–675.
- [10] T. Hama, T. Ohkubo, K. Kurisu, H. Fujimoto, H. Takuda, *Journal of Materials Processing Technology* 177 (2006) 676–679.
- [11] L. Gao, M. Strano, *Journal of Materials Processing Technology* 151 (2004) 294–297.
- [12] M. Plancak, F. Vollertsen, J. Woitschig, *Journal of Materials Processing Technology* 170 (2005) 220–228.
- [13] N.S.P. Varma, R. Narasimhan, A.A. Luo, A.K. Sachdev, *International Journal of Mechanical Sciences* 49 (2007) 200–209.
- [14] P. Ray, B.J. Mac Donald, *International Journal of Mechanical Sciences* 47 (2005) 1498–1518.
- [15] J. Kim, S.W. Kim, W.J. Song, B.S. Kang, *International Journal of Mechanical Sciences* 47 (2005) 1023–1037.
- [16] J.P. Abrantes, A. Szabo-Ponce, G.F. Batalha, *Journal of Materials Processing Technology* 164–165 (2005) 1140–1147.
- [17] W.J. Song, S.W. Kim, J. Kim, B.S. Kang, *Journal of Materials Processing Technology* 164–165 (2005) 1618–1623.
- [18] A. Kulkarni, P. Biswas, R. Narasimhan, A.A. Luo, R.K. Mishra, T.B. Stoughton, A.K. Sachdev, *International Journal of Mechanical Sciences* 46 (2004) 1727–1746.
- [19] J. Kim, B.S. Kang, S.M. Hwang, H.J. Park, *Journal of Materials Processing Technology* 153–154 (2004) 544–549.
- [20] J. Kim, S.W. Kim, W.J. Song, B.S. Kang, *International Journal of Mechanical Sciences* 46 (2004) 1535–1547.
- [21] N. Asnafi, A. Skogsgardh, *Materials Science and Engineering A* 279 (2000) 95–110.
- [22] H.K. Zadeh, M.M. Mashhadi, *Journal of Materials Processing Technology* 177 (2006) 684–687.